Journal of Power Sources 196 (2011) 6099–6103

Contents lists available at ScienceDirect

Journal of Power Sources

journal homepage: www.elsevier.com/locate/jpowsour

Short communication

Effects of tungsten oxide addition on the electrochemical performance of nanoscale tantalum oxide-based electrocatalysts for proton exchange membrane (PEM) fuel cells

Takkeun Oh, Jin Yong Kim*, Yongsoon Shin, Mark Engelhard, K. Scott Weil

Pacific Northwest National Laboratory, 902 Battelle Blvd., Richland, WA 99352, United States

ARTICLE INFO

Article history:
Received 17 January 2011
Received in revised form 23 March 2011
Accepted 26 March 2011
Available online 6 April 2011

Keywords:
PEM
ORR
Tantalum oxide-based catalyst
Non-PGM catalyst

ABSTRACT

In the present study, the properties of non-platinum based nanoscale tantalum oxide/tungsten oxide-carbon composite catalysts were investigated for potential use in catalyzing the oxygen reduction reaction on the cathode side of a PEM fuel cell. All of the tantalum oxide-based catalysts exhibit high ORR on-set potentials, comparable with the commercial Pt/C catalyst even though oxygen reduction current was limited. The tungsten oxide doping to tantalum oxide improved catalytic performance. The performance enhancement was due to a decrease in resistance polarization with increasing tungsten content mainly due to the decrease in resistance polarization. XPS results indicate that the oxidation state of tungsten is +6 and that of the tantalum is +5, suggesting that excess oxygen is generated in the resulting oxide structure. This compositional effect seems to reduce resistance polarization by altering the surface chemistry of the tantalum oxide and enhancing the reaction steps such as surface diffusion. Maximum performance was achieved with a catalyst containing 32 mol% of tungsten oxide, reaching a mass specific current density of ~7% that of the commercial Pt/C catalyst at 0.6 V vs. NHE and ~35% at 0.2 V vs. NHE. In term of area-specific current density, five-fold increase in loading of the doped catalyst leads to a 4–4.5 fold increase in area specific current density at 0.6 V vs. NHE, reaching 66% that of the Pt/C catalyst at 100 rpm and 35% at 2400 rpm.

Published by Elsevier B.V.

1. Introduction

Proton exchange membrane fuel cells (PEMFCs) have the potential to enable efficient, clean power for stationary and transportation applications. However, present-day PEMFC technology falls short on meeting several metrics, including overall system cost. Current PEMFC stacks typically employ platinum-on-carbon catalysts (Pt/C) to dramatically enhance the kinetics of the electrochemical reactions occurring at either electrode. In fact, recent stack costs estimates sponsored by the U.S. Department of Energy indicate that over 30% of the cost of an entire PEMFC stack is directly attributable to the cost of these catalysts, the majority of which is used in the cathode to catalyze the oxygen reduction reaction (ORR) [1,2]. Therefore, development of economical non-Pt based catalysts is critical for the commercialization [1–4]. Any alternatives of Pt catalysts must exhibit the following characteristics: (1) good catalytic activity for the ORR, at least within an order of magnitude of that exhibited by Pt, (2) good electrical conductivity, (3) long-term stability under nominal cell operating conditions in the highly corrosive environment of the stack, and (4) low cost. Several approaches have been attempted to replace Pt/C catalysts, including a heat-treated mixture of transition metal salts and nitrogen-containing precursors [5–9] and ceramic-based catalysts such as transition metal oxide, oxynitride and carbonitride [10–17]. However, none of these catalysts have completely satisfied all the requirements needed for PEM cathode catalysts described above.

Ta_2O_5 is currently under evaluation as an alternative ORR catalyst because of its high oxygen reduction onset potential and excellent stability under corrosive environments [10,18]. Although bulk tantalum oxide exhibits an oxygen reduction potential (~0.95 V vs. NHE) that is comparable to Pt (>1 V vs. NHE), the reduction current is limited due to the poor electrical conductivity of tantalum oxide [18]. Specifically, in the case of a non-conductive catalyst, the desired electrochemical reaction will not take place over the entire surface of the catalyst, but will be limited to triple phase boundary (TPB) regions where the oxide makes a contact with the conductive support and the liquid electrolyte. Thus, measures taken to increase the TPB length, for example by reducing the particle size of the catalyst or increasing the surface area of the conductive support for a given catalyst loading, should improve overall electrocatalytic performance [19–24].

* Corresponding author. Tel.: +1 509 375 2225; fax: +1 509 376 2248.
E-mail address: Jin.Kim@pnl.gov (J.Y. Kim).

0378-7753/$ – see front matter. Published by Elsevier B.V.
doi:10.1016/j.jpowsour.2011.03.058

In our previous publication, it is reported that nanoscale tantalum oxide catalysts prepared using a chemical synthesis technique yielded a more extended, three-dimensional structure of nanoscale tantalum oxide particles on a finely divided carbon powder support and the reduction current increased with decrease in particle size of tantalum oxide [18]. These catalysts exhibited a high ORR onset potential, and displayed some catalytic activity for the ORR.

In the present work, the modification of the defect structure and/or oxidation state was attempted by adding tungsten oxide as a dopant to the nanoscale tantalum oxide catalysts in order to achieve the further enhancement in catalytic performance.

2. Experimental

Carbon-supported nanoscale tantalum oxide-based catalysts were prepared using a chemical synthesis approach that employed tantalum ethoxide [$Ta(OEt)_5$, 99.95%; Alfa Aesar], tungsten ethoxide [$W(OEt)_6$, 99.8% Alfa Aesar], and nanoscale carbon powder (average particle size ~30 nm, Ashbury Carbons, Grade #: 5345R). Carbon powder was functionalized with –OH groups using a previously reported procedure to induce the formation of covalent bonding between oxide and carbon [25]. In all synthesized oxide/carbon composite powders, the content of oxide was ~17 wt%.

The electrode preparation and rotating disc electrode tests were conducted in a similar way described by Suĭarez-Alcĭantara et al. [26]. In all of the electrochemical measurements, a glassy carbon disc (Pine AFE3MGC) with a cross sectional area of 0.196 cm^2 was employed as a test support. The electrocatalyst ink was prepared by mixing 0.6 g of each synthesized compound with 5 mL ethanol and 4 mL of 5 wt% Nafion® (Du Pont, 1100 EW). The resulting mixture was sonicated for 1 min and 5 μL of catalytic ink was deposited onto the glassy carbon surface. For comparison, an electrode of a commercial Pt/C catalyst (Alfa Aasar, 10 wt% Pt) and an electrode containing only nanoscale carbon powder were also prepared following the same procedure. The active solid loading of tantalum-based oxide and Pt/C catalysts was around 0.2 mg cm^{-2}.

The electrochemical measurements were performed at 60 °C using a conventional half-cell test set up with a three-electrode test vessel (Pine AFCELL3). In order to determine the catalytic performance of the synthesized compounds for the ORR, a rotating disc electrode (RDE) with a Pine AFMSRCE rotation speed controller was used. A voltage sweep from 1.1 to 0.2 V vs. NHE at a scanning speed of 5 mV s^{-1} was conducted at a rotation speed in the range of 100–2400 rpm using a potentiostat/galvanostat (Solartron 1287). A gold mesh was employed as a counter electrode, and Hg/Hg_2SO_4/0.5 M sulfuric acid served as a reference electrode. 0.5 M sulfuric acid (pH 3) was used as an electrolyte which was saturated with oxygen by bubbling oxygen into it [26]. To minimize the contamination or the effects of impurities, a new electrolyte solution was used for each electrode.

Microstructural analysis was conducted using a field-emission scanning electron microscope (LEO 982) and a transmission electron microscope (TEM, JEOL2010) to observe the distribution and particle size of the oxide phase in the composite catalyst. The valences of tantalum and tungsten in the catalysts were investigated by X-ray photoelectron spectroscopy (XPS) using a Physical Electronics Quantum 2000 Scanning ESCA microprobe equipped with a 16 element multichannel detection system and a focused monochromatic Al Kα X-ray (1486.7 eV) source.

3. Result and discussion

The kinetics of the oxygen reduction reaction (ORR) strongly depends on the local hydrodynamic conditions to which a catalyst is exposed. In this study, RDE testing was utilized to compare the electrochemical performance of nanoscale tantalum oxide-based catalysts with the commercial Pt/C catalyst. Current–voltage (*I–V*) curves of the type shown in Fig. 1 were used to determine the ORR onset potential, activation polarization loss, and slope of a linear region for each catalyst. As shown in Fig. 2, the ORR onset potential

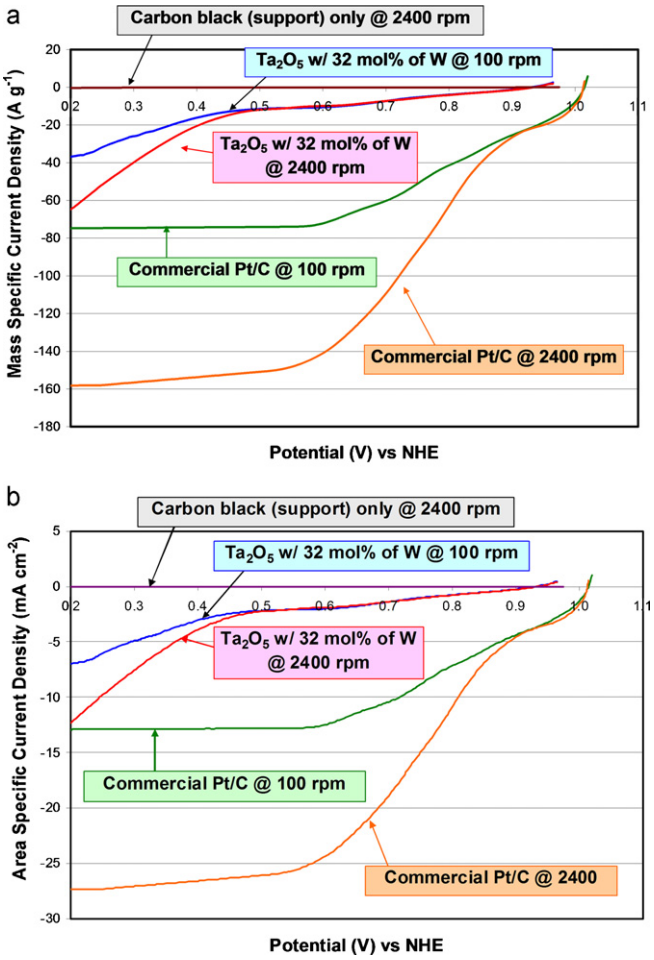

Fig. 1. Voltage sweep curves of a commercial 10 wt% Pt/C (Pt loading: 0.17 mg cm^{-2}) and nanoscale Ta_2O_5 doped with 32 mol% tungsten (oxide loading: 0.18 mg cm^{-2}) measured at 60 °C: (a) mass-specific current density and (b) area-specific current density with respect to NHE.

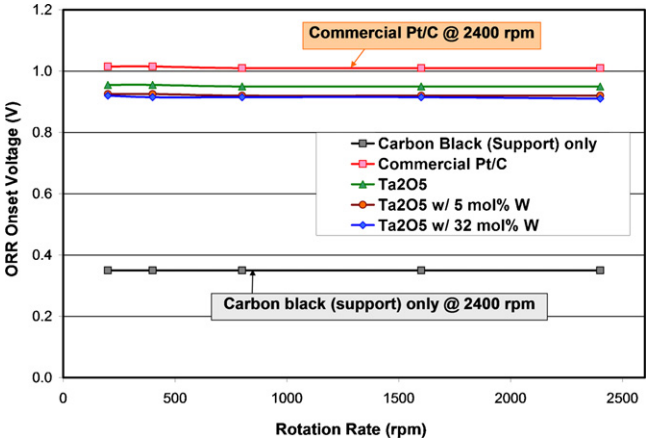

Fig. 2. ORR onset potentials of carbon black, commercial Pt/C and various nanoscale tantalum oxide-based catalysts.

Table 1
Activation polarization loss and resistance polarization calculated from the slope of a linear region in *I–V* curves tested at 60 °C under 2400 rpm rotating speed.

	Pt/C (10 wt% Pt)	Ta_2O_5 (17 wt% oxide)	Ta_2O_5 with 32 mol% W (17 wt% oxide)
Activation polarization loss (V)	0.07	0.46	0.45
Resistance polarization from slope of linear region (Ω g)	0.0022	0.0063	0.0040

defined as the voltage under which the reduction current (negative) is detected, is ~1.01 V vs. NHE for the commercial Pt/C catalyst and is essentially invariant of rotating speed over the range tested. To understand the catalytic activity of catalysts, the activation polarization loss was calculated by extrapolating the linear region of the *I–V* curve to the voltage axis. The difference between the ORR onset potential and the intercept on voltage axis of the extrapolated linear region of the *I–V* curve represents the overpotential required to overcome the activation polarization. In the case of the commercial Pt/C catalyst, this difference, activation polarization loss, is quite small (0.07 V) as reported in Table 1. In the voltage range above 0.9 V vs. NHE, the reduction current was invariant to rotating speed since the activation polarization is the dominant in this range. At potentials lower than 0.8 V where linear resistance polarization loss was observed, the slope increased with higher rotating speeds and reached a limiting current at ~0.55 V vs. NHE.

As reported by Kim et al. [18] and Ishihara et al. [10], tantalum oxide revealed high ORR onset potential. The tantalum oxide-based catalysts doped with *W* up to 32 mol% also exhibited a high ORR onset potential of ~0.94 V vs. NHE that remained unchanged as a function of rotating speed (see Fig. 2). To confirm the electrochemical activity of the tantalum oxide-based catalyst, an electrode containing the equivalent weight of carbon powder support alone was prepared and tested in the same condition. The carbon support itself displays a very low ORR onset potential (0.35 V vs. NHE, Fig. 2) and negligible current density due to double layer capacitance (see Fig. 1). These results indicate that the ORR onset potential and current exhibited by the tantalum oxide-based catalyst is indeed due to the catalytic activity of the oxide phase. Unlike the Pt/C catalyst, a large activation polarization loss of 0.45–0.46 V was observed in the nanoscale tantalum oxide-based catalyst (refer to Table 1). A representative back-scattered SEM image and a bright field TEM image are shown in Fig. 3. These images show that oxide agglomerates, which are ~20 nm in size, are uniformly distributed on carbon supports. Despite their small size, the tantalum oxide-based catalyst is still not as active as the commercial Pt/C catalyst. At potentials less than 0.4 V vs. NHE, the tantalum oxide-based catalyst started to show a linear region dominantly caused by resistance polarization. No diffusion limitation was observed over the lower potential range studied. Since no limiting current was observed on tantalum oxide-based catalysts, no detailed kinetic study was conducted for these catalysts in this study.

Plotted in Fig. 4(a) and (b) are the relative mass specific current densities at 0.6 V vs. NHE and the maximum mass specific current densities (measured at 0.2 V vs. NHE) for three different nanoscale tantalum oxide-based catalyst compositions in comparison with the Pt/C. The relative mass specific current density at 0.6 V vs. NHE decrease as a function of rotating speed. In general, the high rotating speed of an electrode creates a thinner layer for oxygen diffusion and a corresponding higher oxygen gradient, which minimizes the oxygen diffusion barrier in the electrolyte solution. While the baseline Pt/C catalyst exhibited an linear increase in reduction current at 0.6 V vs. NHE and the electrochemical performance was improved with increasing rotating speed (refer to Fig. 1), the *I–V* curves of nanoscale tantalum oxide-based catalysts were dominantly influenced by activation polarization at this potential, in which the reaction kinetics is not sensitive to oxygen diffusion and rotating speed. Therefore, the relative mass specific current density of oxide-based catalysts decreased with rotating speed at this potential.

Also observed in Fig. 4(a) and (b), the mass specific current density increases with increasing tungsten content, achieving a maximum for the 32 mol% tungsten-doped catalyst. The best performance at 0.6 V vs. NHE is ~7% of the mass specific current density of Pt/C at 2400 rpm. At 0.2 V vs. NHE, this catalyst exhibits a maximum mass specific current density of 50% that of the Pt/C catalyst at low rotating speed (100 rpm) and 35% at the highest speed (i.e. under minimal oxygen diffusion effects). The improvement observed in the tungsten-doped catalysts is related to a corresponding decrease in resistance polarization indicated by the slope of a linear region in *I–V* curves. Compared in Table 1 are the activation polarization loss and the resistance polarization slope of doped and undoped tantalum oxide catalysts at 2400 rpm. The activation polarization losses do not change significantly with the addition of tungsten, while the slope of the linear region increases and the corresponding resistance polarization (the reciprocal of the slope) decreases from 0.0063 Ω g for the undoped catalyst to 0.0040 Ω g for the 32 mol% tungsten-doped material.

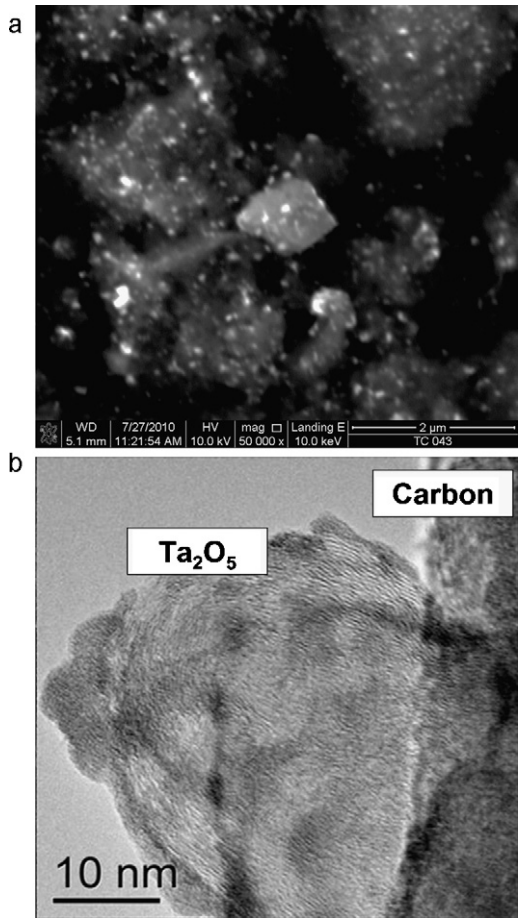

Fig. 3. (a) SEM back-scattered electron image and (b) TEM bright-field image conducted on the carbon-supported nanoscale tantalum oxide catalyst.

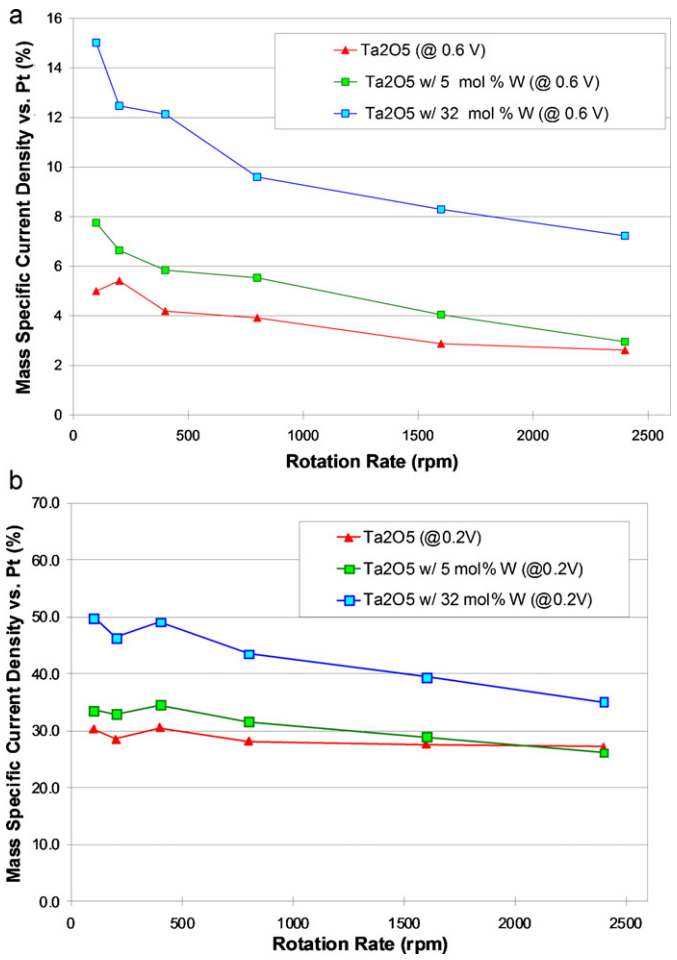

Fig. 4. Mass specific current density of nanoscale tantalum oxide-based catalysts compared to Pt/C catalyst: (a) at 0.6 V vs. NHE and (b) at 0.2 V vs. NHE (maximum mass specific current density).

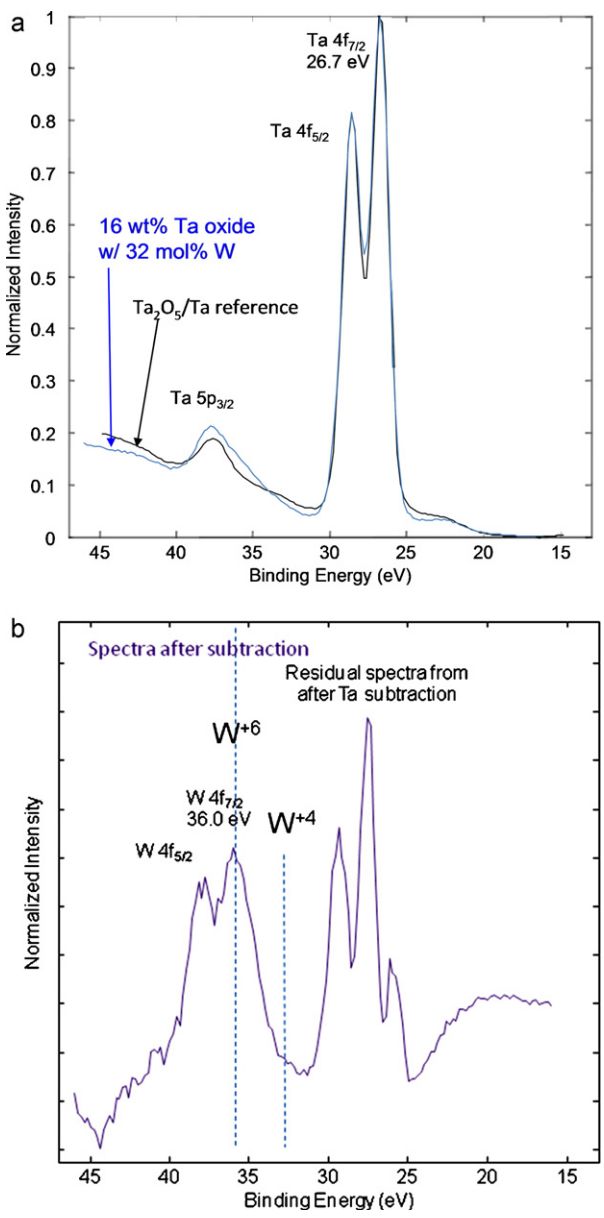

Fig. 5. XPS spectra of tantalum oxide catalyst with 32 mol% tungsten: (a) normalized overlay plot with Ta_2O_5 reference and (b) spectra after subtracting the normalized intensity of Ta_2O_5 from the spectra of the sample.

To understand the role of tungsten in tantalum oxide structure, the valences of the tantalum and tungsten cations in the 32 mol% tungsten-doped catalyst were examined by XPS. The XPS spectra shown in Fig. 5(a) are the normalized overlay plot of the sample compared with Ta_2O_5 reference in which the oxidation state of tantalum cation is +5. A close match of two spectra indicates that the oxidation state of tantalum in the sample is also +5. To figure out the oxidation state of tungsten in the sample, the spectra of the reference Ta_2O_5 was subtracted from the spectra of the sample (see Fig. 5(b)). This spectra show that the oxidation state of the tungsten in the tantalum oxide-based catalyst is +6, suggesting that the addition of +6 tungsten cations generates excess oxygen anions in the tantalum oxide structure. These excess oxygen anions can enhance surface transport mechanisms such as surface diffusion. Thus, the improvement observed in the catalytic performance of tungsten-doped catalysts appears to be related to the formation of excess oxygen in the tantalum oxide structure, which can decreases the resistance polarization caused by surface phenomena such as surface diffusion.

Shown in Fig. 6 is a comparison of the area-specific current densities of the undoped tantalum oxide catalyst, the 32% tungsten-doped catalyst at a loading of 0.18 mg cm^{-2}, and the same doped catalyst at higher loadings (0.38 mg cm^{-2} for two times loading and 0.94 mg cm^{-2} for five times loading) with the baseline Pt/C catalyst (0.17 mg cm^{-2} Pt loading). The increase in loading for the doped catalyst leads to a 4–4.5 fold increase in area specific current density at 0.6 V vs. NHE, reaching 66% that of the Pt/C catalyst (at a loading of 0.17 mg of Pt per unit area cm^2) at 100 rpm and 35% at 2400 rpm. Thus, even though the inherent catalytic performance of the tungsten-doped catalyst is an order of magnitude lower than that of Pt/C due to a large activation polarization, the substantially lower cost of the oxide-based catalyst (by several orders of magnitude) allows for higher loadings and in turn mass and area specific current densities on the same order as Pt/C. That is, the tungsten-doped, carbon-supported nanoscale tantalum oxide catalyst can be potentially an economically viable, non-Pt alternative for the PEMFC application, especially if their activation polarization can be reduced further. Additional dopant studies as well as a process development effort to produce the smaller oxide particles are planned to understand if greater reductions in the activation polarization of tantalum oxide-based catalysts are possible.

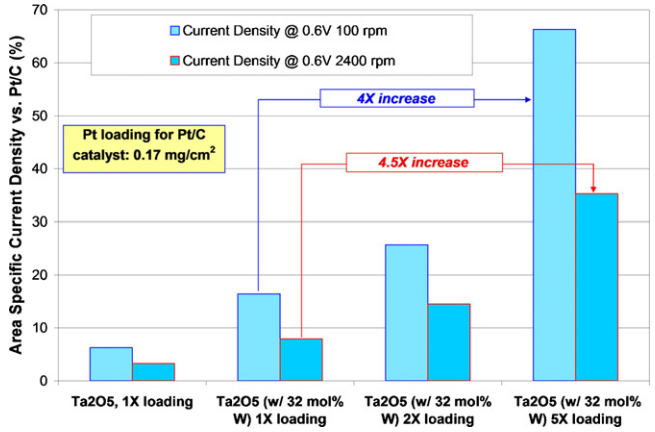

Fig. 6. Area specific current density of various tantalum oxide catalysts compared to Pt/C catalyst. The standard loading of active materials (1*X*) was 0.21 mg cm^{-2} for undoped tantalum oxide, 0.18 mg cm^{-2} for 32 mol% W-doped tantalum oxide, and 0.17 mg cm^{-2} for the commercial Pt/C catalyst, respectively. For higher loading of 32 mol% W-doped tantalum oxide, 2*X* and 5*X* loadings represent 0.38 mg cm^{-2} and 0.94 mg cm^{-2}, respectively.

4. Conclusions

The ORR properties of tungsten-doped tantalum oxide-based catalysts were studied using a half-cell rotating disc electrode set up. Relative to the undoped tantalum oxide catalyst, the tungsten-doped materials displayed a substantial improvement in electrochemical performance with little change in the ORR onset potential. At 0.6 V vs. NHE, the mass specific current density of the 32 mol% tungsten-doped catalyst reached ~15% that of a baseline 10 wt% Pt at a RDE speed of 100 rpm and ~7% at 2400 rpm. The performance enhancement was due to a decrease in resistance polarization with increasing tungsten content. XPS results indicate that the oxidation state of tungsten is +6 and that of the tantalum is +5, suggesting that excess oxygen is generated in the resulting oxide structure. It is speculated that this compositional effect reduces resistance polarization by altering the surface chemistry of the tantalum oxide. By increasing the loading of the active material five fold, it was shown that the area specific current density of these materials could be increased to 35% that of the baseline Pt/C catalyst at 2400 rpm. Even though the electrochemical activity of tantalum-oxide based materials are significantly lower than Pt catalysts, the low cost of tantalum oxide and respectable area-specific current density with high loading demonstrate the potential of these nanoscale composite oxide-based catalysts as potential Pt-free alternatives for use in catalyzing the ORR in PEMFC cathodes.

Acknowledgments

This work was supported by Pacific Northwest National Laboratory (PNNL) lab-directed research and development (LDRD) program. The XPS and TEM studies were performed using EMSL, a national scientific user facility sponsored by the Department of Energy's Office of Biological and Environmental Research and located at Pacific Northwest National Laboratory. PNNL is operated by Battelle Memorial Institute for the United States Department of Energy (U.S. DOE) under contract DE-AC06-76RLO 1830.

References

[1] H. Gasteiger, M. Mathias, in: M. Murthy, F.T. Fuller, J.W. Van Zee, S. Gottesfield (Eds.), Proton Conducting Membrane Fuel Cells III, PV2002-31, The Electrochemical Society Inc., 2005, p. 1.
[2] E.J. Carlson, P. Kopf, S. Sriramulu, Y. Yang, Cost Analyses of Fuel Cell Stack/Systems, U.S. Department of Energy 2006 Hydrogen Annual Report, 2006, V.G.9.
[3] C. Jaffray, G.A. Hards, in: W. Vielstich, A. Lamm, H. Gasteiger (Eds.), Handbook of Fuel Cells—Fundamentals, Technology and Applications, vol. 3, Wiley & Sons, Chichester, UK, 2003, p. 509.
[4] S. Lister, G. McLean, J. Power Sources 130 (2004) 61.
[5] H.-J. Zhang, Q.-Z. Jiang, L. Sun, X. Yuan, Z.-F. Ma, Electrochim. Acta 55 (2010) 1107.
[6] S.Y. Ye, A.K. Vijh, Electrochem. Commun. 5 (2003) 272.
[7] M. Yuasa, A. Yamaguchi, H. Itsuki, K. Tanaka, M. Yamamoto, K. Oyaizu, Chem. Mater. 17 (2005) 4278.
[8] R. Bashyam, P. Zelenay, Nature 443 (2006) 63.
[9] H. Liu, Z. Shi, J. Zhang, L. Zhang, J. Zhang, J. Mater. Chem. 19 (2009) 468.
[10] A. Ishihara, M. Tamura, K. Matsuzawa, S. Mitsushima, K. Ota, Electrochim. Acta 55 (2010) 7581.
[11] A. Ishihara, S. Doi, S. Mitsushima, K. Ota, Electrochim. Acta 53 (2008) 5442.
[12] Y. Ohgi, A. Ishihara, Y. Shibata, S. Mitsushima, K. Ota, Chem. Lett. 37 (2008) 608.
[13] Y. Liu, A. Ishihara, S. Mitsushima, N. Kamiya, K. Ota, J. Electrochem. Soc. 154 (2007) B664.
[14] J.-H. Kim, A. Ishihara, S. Mitsushima, N. Kamiya, K. Ota, Electrochim. Acta 52 (2007) 2492.
[15] Y. Maekawa, A. Ishihara, S. Mitsushima, K. Ota, Electrochem. Solid-State Lett. 11 (2008) B109.
[16] J.-H. Kim, A. Ishihara, S. Mitsushima, N. Kamiya, K. Ota, Electrochemistry 75 (2007) 166.
[17] A. Ishihara, Y. Sibata, S. Mitsishima, K. Ota, J. Electrochem. Soc. 155 (2008) B400.
[18] J.Y. Kim, T. Oh, Y. Shin, J.F. Bonnet, K.S. Weil, Int. J. Hydrogen Energy 36 (2011) 4557.
[19] T. Ushikubo, Catal. Today 57 (2000) 331.
[20] F. Cardarelli, P. Taxil, A. Savall, C. Comninellis, G. Manoli, O. Leclerc, J. Appl. Electrochem. 28 (1998) 245.
[21] Z. Sun, H.C. Chiu, A.C.C. Tseung, Electrochem. Solid-State Lett. 4 (2001) E9.
[22] J. Ribeiro, A.R. De Andrade, J. Electrochem. Soc. 151 (2004) D106.
[23] A. Bonakdarpour, R. Lobel, S. Sheng, T.L. Monchesky, J.R. Dahn, J. Electrochem. Soc. 153 (2006) A2304.
[24] P. Jain, J.S. Juneja, V. Bhagwat, E.J. Rymaszewski, L. Toh-Ming, T.S. Cale, J. Vac. Sci. Technol. A 23 (2005) 512.
[25] Y. Shin, J.Y. Kim, J.F. Bonnett, K.S. Weil, Surf. Sci. 603 (2009) 2290.
[26] K. Suĭarez-Alcĭantara, A. Rodrĭguez-Castellanos, R. Dante, O. Solorza-Feria, J. Power Sources 157 (2006) 114.